

## **VELOCITY MEASUREMENTS IN THE NEAR NOZZLE REGION OF COMMON-RAIL DIESEL SPRAYS AT ELEVATED BACK-PRESSURES**

Ph. Leick\*, G. Bittlinger\*, C. Tropea<sup>o</sup>

\*Robert Bosch GmbH, Dept. FV/SLE, PO Box 10 60 50, 70049 Stuttgart, Germany

E-Mail: [philippe.leick@de.bosch.com](mailto:philippe.leick@de.bosch.com)

<sup>o</sup>Fachgebiet Strömungslehre und Aerodynamik (SLA)

Technische Universität Darmstadt, Petersenstraße 30, 64287 Darmstadt, Germany

### **ABSTRACT**

The injection system of a modern direct injection Diesel engine plays an important role on the mixture preparation, hence on power, fuel consumption and emissions, which are directly influenced by the atomisation of the spray in the engine cylinder. Detailed knowledge of the interaction between the liquid spray and the surrounding gas is necessary in order to understand the atomisation process, and is required by modern CFD codes to provide boundary conditions for the simulations and to validate them.

However, the high density, high speed and small dimensions of these sprays make measurements of their properties extremely difficult, especially in the primary break-up region close to the nozzle outlet, and quantitative data is therefore still rare. Previous authors have reported the use of Laser Correlation Velocimetry (LCV) to measure spray velocities close to the nozzle exit under atmospheric conditions. For the investigations presented here, the LCV setup was adapted in order to make velocity measurements at elevated back-pressures possible. Time-resolved velocity measurements were performed in the primary break-up region of Common-Rail Diesel sprays, and the results demonstrate that the density of the surrounding gas has a significant direct influence on spray atomisation.

### **INTRODUCTION**

The injection system of a modern direct injection (DI) Diesel engine plays an important role on the mixture preparation, hence on power, fuel consumption and emissions, which are directly influenced by the atomisation of the spray in the engine cylinder. Detailed knowledge of the interaction between the liquid spray and the surrounding gas is necessary in order to understand the atomisation process, and is required for validation of modern CFD codes and to provide initial/boundary conditions for predictions. However, the exact influence of the injection system and injection parameters on the spray breakup is not yet fully understood. It is well known that spray atomisation is not solely controlled by interfacial forces between the liquid fuel and the surrounding gas. The breakup behaviour close to the nozzle exit (*primary breakup*) is rather a result of the internal flow conditions at the nozzle exit, such as velocity profile, turbulence and cavitation. These issues are responsible for initiating first perturbations on the spray surface. These first perturbations are the basis for further breakup processes (*secondary breakup*) being controlled by the intensity of momentum exchange with the surrounding gas phase. Consequently all other subsequent processes such as evaporation, spray/wall interaction with the piston bowl, ignition and finally combustion are dependent on the primary spray atomisation [1].

Quantitative experimental data about spray properties close to the nozzle exit is difficult to obtain, the high speeds and microscopic dimensions of the fuel jets making the application of most measurement techniques extremely challenging. High-speed photography has been used extensively to characterise Diesel sprays, but can only reveal information about the spray surface, which contains only a small fraction of the total injected fuel mass [2]. The phase Doppler technique has previously been used to measure droplet velocities in high-pressure Diesel sprays, but its range is limited to distances from the nozzle exit well above the spray's breakup length [3, 4, 5]. Laser Correlation Velocimetry (LCV, or Laser-2-Focus-Velocimetry), a technique originally developed to measure velocities in seeded gas flows [6, 7], has been adapted by Chaves [8] for application in dense sprays. LCV is well suited for velocity measurements close to the nozzle exit, but only under atmospheric conditions. With typical distances between spray and optics of around 10 mm in these experiments [9], it is clear that a straightforward adaptation of these techniques to measure the velocities of sprays injected inside a pressure vessel is not possible. However, the properties of the medium into which the fuel is injected have considerable influence upon the generation and propagation of the spray. It is therefore desirable to modify the LCV technique in such a way that velocities can be measured in the dense primary breakup zone of a Diesel spray injected into a gas whose density and/or back pressure approximate typical conditions found in a DI Diesel engine at the time of injection.

## EXPERIMENTAL SETUP

### Working Principles of Laser Correlation Velocimetry

Laser Correlation Velocimetry (LCV) is an application of the time-of-flight measurement principle [6] to dense liquid sprays. Light coming from two distinct illuminated points in the spray, the detection volumes (DV), is observed and recorded. The intensity of this light exhibits rapid fluctuations as spray structures, such as ligaments, free droplets or cavitation zones cross the detection volumes. The signal from the second DV, which is located slightly downstream of the first, will be similar in appearance to the one from the first DV, since any structure passing the first DV has a high probability of also passing the second one. The first signal therefore leads the second one by a small time delay  $\Delta t$ , which, in conjunction with the known distance  $\Delta x$  between the two detection volumes, is used to calculate the spray velocity  $v$  as  $v = \Delta x / \Delta t$ . If the size of the detection volumes and their separation are sufficiently small, LCV can be considered to be a point-measurement technique.

The apparent simplicity of LCV is its main advantage and accounts for its ability to measure spray velocities in dense sprays. There are no restrictions on nature, size, shape or concentration of the tracer structures, and the only parameter that needs to be precisely determined is  $\Delta x$ , which is not difficult to measure.

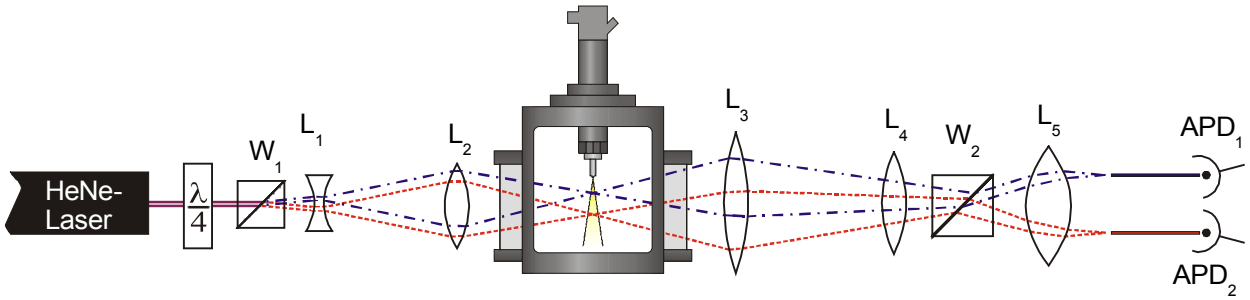


**Figure 1:** Setup of the optical system used for LCV: the focal points of two laser beams are used as detection volumes.

A detailed overview of the optical system used at Bosch's LCV test rig to create the detection volumes and collect the light coming from them is given in Figure 1. The beam from a cw-HeNe-Laser is split into two beams with a very low separation angle ( $0^\circ 10'$ ) by the Wollaston prism  $W_1$ . The intensity of both beams is approximately equal, since the laser light's polarisation is changed from linear to circular using a quarterwave plate ( $\lambda/4$ ). The two beams are then expanded by a first lens  $L_1$  and focused into the centre of the chamber by a second lens  $L_2$ , thus creating the two small detection volumes. Prior beam expansion is necessary in order to minimise the size of the foci: if the laser beams entering the focusing lens ( $L_2$ , focal distance  $f_2$ ) are parallel or nearly parallel and have a  $1/e^2$ -radius  $w_2$ , the beam waists in the focus are given by

$$w_0 = \frac{\lambda f_2}{\pi w_2}, \quad (1)$$

$\lambda$  being the laser wavelength [10]. The lens  $L_2$ 's focal length  $f_2$  is then also the distance between the focusing lens and the focal points. It is therefore desirable to keep  $f_2$  small (which requires a very compact pressure vessel) and to increase  $w_2$ . In the setup of Figure 1, to save space, the laser beams, which are divergent after passing  $L_1$ , are not parallelised before being focused into the chamber. However, Eq. (1) is still a useful approximation of the relationship between the beam radius in the focus and the properties of the focusing lens.

To collect the light coming from the DVs using two different detectors, the separation between the two beams needs to be increased, which is done using a second Wollaston prism  $W_2$ . The DVs are mapped into these detectors (Avalanche Photodiodes, or APDs) by the optical system consisting of the lenses  $L_3$ ,  $L_4$  and  $L_5$ .

### Test-Rig Description

The test-rig on which the LCV experiments are carried out is based on a Common-Rail application. Standard calibration oil, whose properties (especially density, viscosity, surface tension) are very similar to those of Diesel fuel, but specified within a narrower range, is used. Rail pressures up to 135 MPa are provided by a CP1 pump. The pressure vessel (Figure 2) is mounted on a traversing table equipped with stepper motors and can thus be moved freely in the horizontal plane. The position of the detection volumes along the vertical direction can be adjusted by moving the optics focusing the laser light into the pressure chamber. This makes velocity profile measurements at different distances from the nozzle exit possible.

The distance between the two focal points, located in the centre of the pressure vessel, was measured to be  $\Delta x = 70.5 \mu\text{m}$ , the  $1/e^2$ -beam diameters were estimated at  $2w_0 \approx 12 \mu\text{m}$ , which is sufficiently small to resolve the spatial structures of the spray.

The signals from both APDs are amplified and frequency filtered using a band-pass filter (with -3dB points at 64 kHz and 4 MHz), then recorded using a digital storage oscilloscope with 8-bit resolution at a sampling rate of 100 MHz. Subsequently, these records are transferred to a computer for evaluation, where they are divided into small

time windows, for each of whom the time delay between the signals is calculated using a cross correlation algorithm ([9], a detailed description of the evaluation and validation method can also be found in [11], an error-analysis is carried out in [12]).

The pressure vessel and spray traps were designed in such a way that they can accommodate three-hole nozzles, which are a good approximation of standard multi-hole nozzles. However, a one-hole nozzle oriented in forward direction was used for the first experiments with this test-rig, which will be presented in the following sections. The nozzle diameter at the outlet is  $154 \mu\text{m}$ , the spray hole itself has a k-factor and a high degree of hydrogrinding. Energisation timing of the solenoid valves was chosen in such a way that maximum needle lift was just achieved.

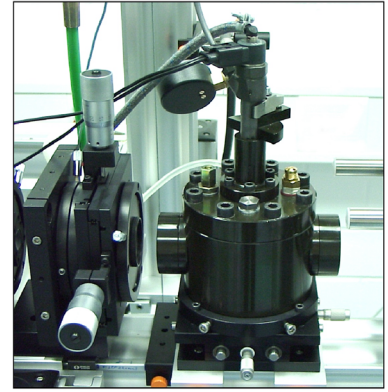


**Figure 2:** LCV pressure vessel; the total length of the chamber along the optical axis is 150 mm, maximum back-pressure is  $p_B = 5 \text{ MPa}$ . Spray traps inhibit the deposition of fuel droplets on the windows, and fog formation is prevented by a continuous gas flow inside the chamber. Changes of the refractive index of the chamber gas, which is proportional to its density, are compensated by an appropriate correction of the chamber position along the optical axis.

## RESULTS

In the following section, velocity measurements conducted under identical conditions, except for the injection pressure  $p_I$  and back-pressure  $p_B$ , which has been varied between atmospheric conditions and 2 MPa of pure  $\text{N}_2$  at room temperature (corresponding to a gas density of  $\rho_g = 23 \text{ kg/m}^3$ , typical for diesel engines near top-dead centre at high part-load conditions), are presented. For first investigations, the injection pressure was chosen as low as possible ( $p_I = 22 \text{ MPa}$ ), resulting in the best possible signal-to-noise ratio. Further investigations were conducted at  $p_I = 80 \text{ MPa}$ , a typical injection pressure at part-load in Common-Rail Diesel engines.

### Velocity Measurements at $p_I = 22 \text{ MPa}$ , $p_B = 0.1 \text{ MPa}$ and $p_B = 2 \text{ MPa}$

Figure 3 shows velocities recorded at different distances  $r$  from the spray axis and at different back-pressures  $p_B$ . Each data point shown is an average calculated from 30 different injections, the error bars represent the standard deviations. Corresponding shadow images of the sprays are depicted in Figures 4, 5. The appearance of the fuel jets emerging from the nozzle exit is not different for the two investigated back-pressures. Since large-scale cavitation does not occur in the spray hole under the investigated conditions, it seems reasonable to conclude that the nozzle flow is not qualitatively different for  $p_B = 0.1$  and 2 MPa. However, the influence of the surrounding medium on spray atomisation is obvious, as both the length of the undisturbed liquid column is shortened and the size of the structures separated from the spray core is reduced at elevated back-pressure.

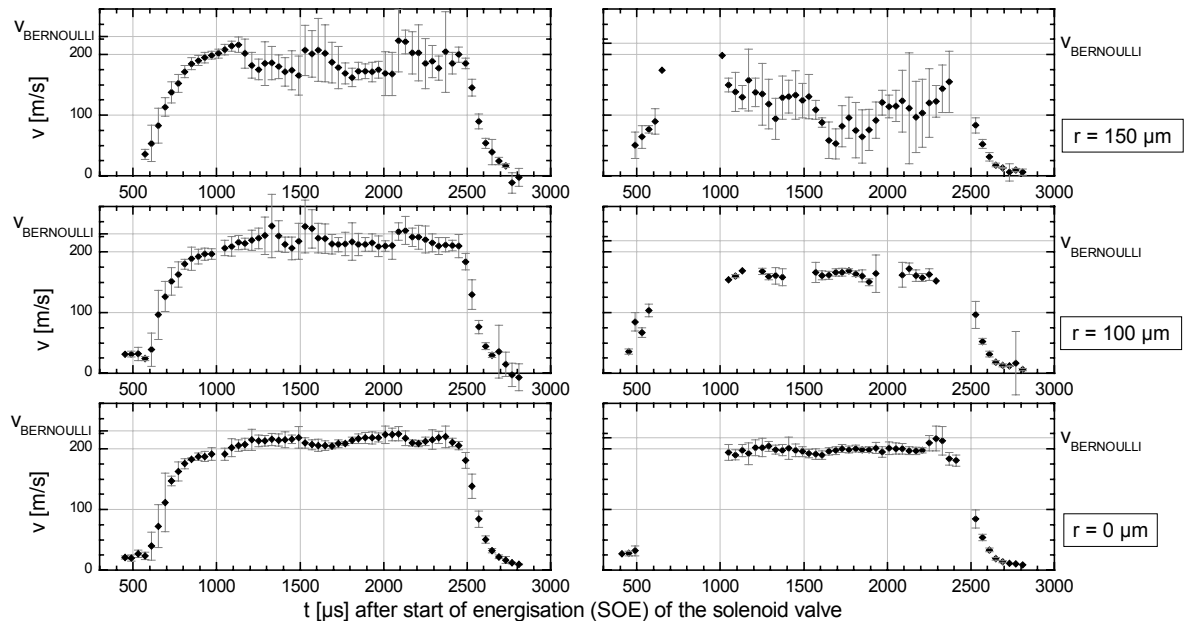


**Figure 3:** Spray velocities as a function of time,  $p_I = 22 \text{ MPa}$ ,  $h = 1.9 \text{ mm}$ , at  $p_B = 0.1 \text{ MPa}$  (left column) and  $p_B = 2 \text{ MPa}$  (right column), for different distances  $r$  from the spray axis. At elevated back-pressure, signal-to-noise ratios were too low at the beginning of injection ( $t = 500\text{-}1000 \mu\text{s}$ ), making valid velocity measurements impossible.

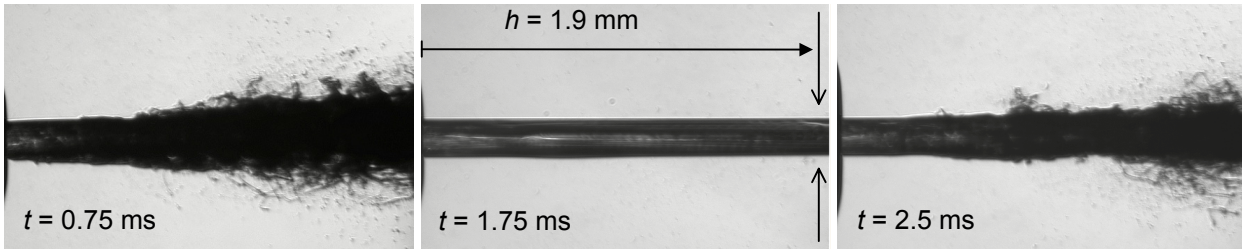


**Figure 4:** Shadow images of the spray,  $p_B = 0.1$  MPa, at the beginning, during steady-state and at the end of injection.

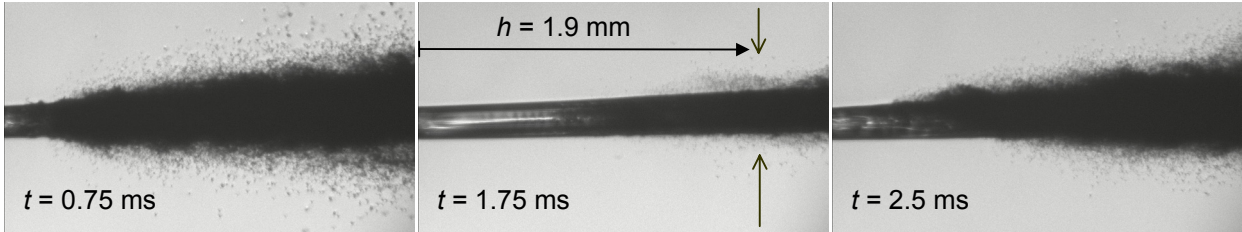


**Figure 5:** Shadow images of the spray,  $p_B = 2$  MPa, at the beginning, during steady-state and at the end of injection.

The rapid rise and drop of spray velocities at the beginning and end of the injections is due to the fact that, for a short moment during the opening and closing phases of the needle, the spray hole is not the narrowest effective flow area (needle throttling, Figures 4, 5 at  $t = 0.75$  and  $2.5$  ms). During the quasi-steady-state phase of the injection, at full needle lift (around  $t \approx 1.75$  ms), the velocity reaches a value close to  $v_{BERNOULLI}$ . This velocity corresponds to a lossless exit from the nozzle, and it is also shown in the diagrams (Fig. 3). The speeds measured in the dense spray core are much higher than the maximum spray tip velocities shown in Figure 6a. The large shot-to-shot fluctuations of measured velocities that are observed in the dilute region beyond the spray boundary at  $r = 150 \mu\text{m}$  (Figures 3, 4, 5), especially between  $t = 1$  and  $2.4$  ms, where maximum velocities are detected near the dense spray core ( $|r| \leq 100 \mu\text{m}$ ), can be attributed to droplets that have been separated from the main spray.

### Velocity Profiles at $p_I = 22$ MPa, $h = 1.9$ mm

Velocity profiles are obtained by plotting the average spray velocity during a given time period for different radial distances from the spray axis (Figure 6b). Comparing the profiles recorded under atmospheric conditions and in dense atmospheres, it becomes apparent that the region close to the spray axis with near constant velocity is narrower and no longer symmetric around  $r = 0$  at elevated back pressure. Secondary breakup tends to amplify any irregularities of the nozzle flow; greater asymmetries should therefore be expected at higher gas densities. The velocity gradients in the interaction zone are steeper: droplets detected at higher distances from the spray axis have been separated from the main spray for a larger amount of time, and have therefore lost more speed due to drag in the dense gas.

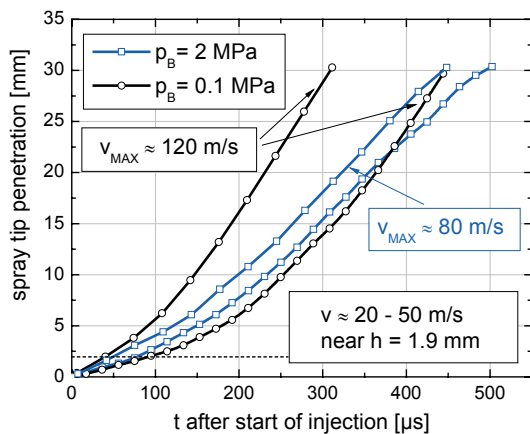


**Figure 6a:** Spray tip penetration at  $p_I = 22$  MPa (for every value of  $p_B$ , high-speed videos from two distinct injections were evaluated). Velocity measurements at  $h = 1.9$  mm are in good agreement with LCV values (first detected velocity for each of the curves of Figure 3).

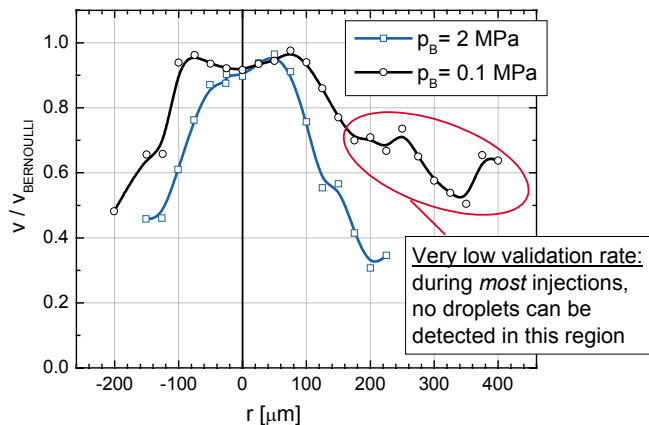


**Figure 6b:** Velocity profiles for  $p_I = 22$  MPa (averaged between  $t = 1.5$  and  $2$  ms),  $h = 1.9$  mm. With  $v_{BERNOULLI} > 200$  m/s, velocities measured in the dense spray using LCV are much higher than the maximum spray tip velocities.

## Velocity Measurements in the Spray-Gas Boundary at $p_I = 80$ MPa, $p_B = 0.1$ and 2 MPa

At an injection pressure of  $p_I = 80$  MPa, it was not possible to measure complete velocity profiles of the spray (Figure 7b). Both under atmospheric conditions and at elevated back pressure, the signal-to-noise ratio in the dense regions near the spray axis ( $r \rightarrow 0$ ) was too low. Velocity data is only available for the dilute regions near and beyond the spray-gas interface, which extend to much larger distances  $r$  from the spray axis than at  $p_I = 22$  MPa. However, even the velocities measured in these regions are much higher than the maximum spray tip velocities (Figure 7a.) The missing velocity data near the centre of the spray make interpretations of the remaining data more difficult, as the exact location of the spray axis is unclear. Backlit images of the spray (Figs. 8a1, 8b1) and root-mean-square (RMS) images of different injections show that the dense spray core (bright areas in 8a2, 8b2) has a slightly higher cone-angle at  $p_B = 2$  MPa, which explains why valid LCV measurements could be found farther from the spray axis at  $p_B = 2$  MPa.

Both the LCV results and the backlit images show significant differences between the atomisation zones beyond the dense spray: under ambient conditions, the optical density is lower than at high  $p_B$ , but the width of the interaction zone is much higher. The velocity gradient is much steeper at high  $p_B$ . As in the previously discussed cases with  $p_I = 22$  MPa, this is caused by higher aerodynamic drag.

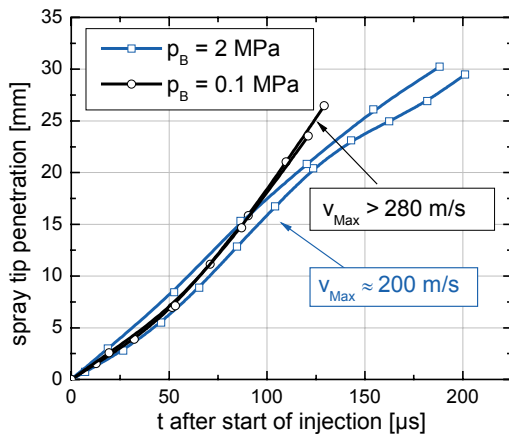


**Figure 7a:** Spray tip penetration for  $p_I = 80$  MPa. The measured spray tip velocities are much lower than the velocities measured near the spray boundary ( $v_{BERNOULLI} > 430$  m/s). An increase of the spray tip velocity is not expected at higher distances from the nozzle exit [14].

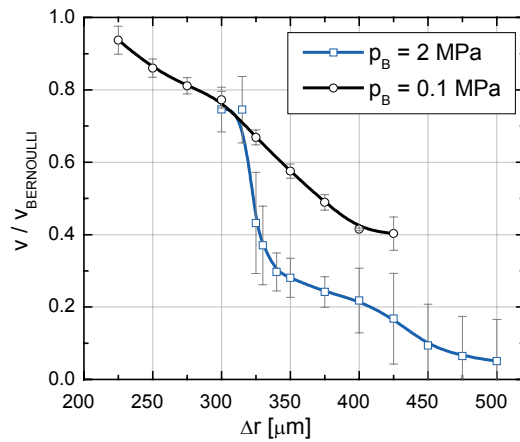


**Figure 7b:** Velocity profiles for  $p_I = 80$  MPa,  $h = 1.9$  mm, at full needle lift.

For  $p_B = 2$  MPa, the velocity gradient is much lower for  $\Delta r \geq 340$   $\mu\text{m}$  – just beyond the interaction zone of Figure 8a2 – than in the interaction zone, around  $\Delta r = 320$   $\mu\text{m}$ . The velocity fluctuations in this region are very high, but unlike in the case  $p_I = 22$  MPa (especially at  $p_B = 0.1$  MPa), discussed previously, where the fluctuations were due to shot-to-shot variations, the velocities change drastically from one time window to the next, within one single injection. The shadow images show practically no droplets in this region, which suggests that the velocities detected there by LCV should be attributed to small droplets (radius  $< \sim 1$   $\mu\text{m}$ ) that have been separated from the dense spray for a sufficiently long time to lose most of their velocity.

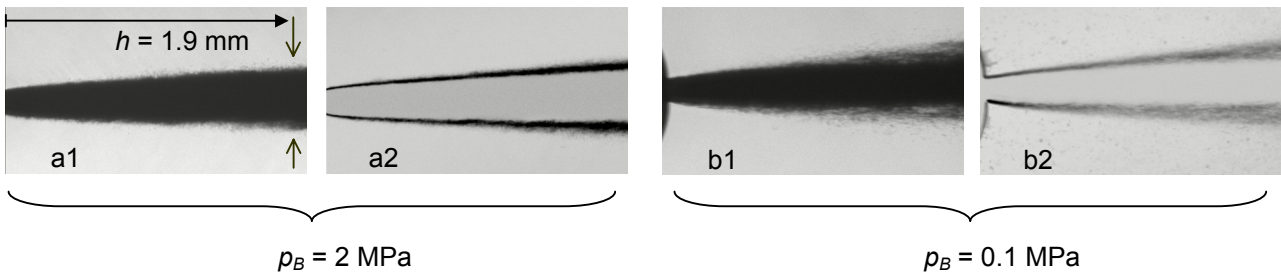


**Figure 8:** Shadow images of the spray, at  $p_I = 80$  MPa, full needle lift.

a2 and b2 are root-mean-square images, where darker areas indicate higher shot-to-shot variations. The dark lines around the spray core correspond to the regions of highest spray-gas interaction. The narrow interaction zone in a2 corresponds to the region with the highest velocity gradient in Figure 7b, at 2 MPa back-pressure.

## SUMMARY

The investigations presented here have proven that, using the described LCV implementation, velocity measurements under high back-pressure conditions in the dense primary breakup zone of a Diesel spray are feasible. These results are complemented by high-resolution spray images, as LCV alone gives no unambiguous information about the density of the spray, which is essential for an in-depth interpretation of the atomisation process. The experiments carried out until now do not yet cover the full parameter range ( $p_I$ ,  $p_B$ , location of the DV) of Diesel applications. In some cases, it has not been possible to perform valid measurements due to insufficient signal-to-noise ratios. Further improvements in the recording equipment and in the methods to evaluate the APD signals are necessary in order to perform velocity measurements at higher  $p_I$  and in sprays of even higher density (i.e. closer to the nozzle exit and to the spray axis).

## LIST OF SYMBOLS

Symbol	[SI unit]	Description	Symbol	[SI unit]	Description
$f$	[mm]	focal length	$v_{BERNOULLI}$	[m/s]	Bernoulli velocity
$h$	[mm]	axial distance from nozzle exit	$v_{Max}$	[m/s]	maximum (spray tip) velocity
$p_B$	[MPa]	chamber back pressure	$w_0, w_2$	[ $\mu$ m]	beam waists ( $1/e^2$ -radius)
$p_I$	[MPa]	fuel injection pressure	$\Delta t$	[ $\mu$ s]	time-delay
$r, \Delta r$	[ $\mu$ m]	radial distance from spray axis	$\Delta x$	[ $\mu$ m]	separation of the detect. vols.
$t$	[ms]	time after start of energisation	$\lambda$	[nm]	laser wavelength
$v$	[m/s]	axial (spray) velocity	$\rho_g$	[kg/m <sup>3</sup> ]	chamber gas density

## REFERENCES

1. G. Bittlinger, O. Heinold, D. Hertlein, T. Kunz and F. Weberbauer, Die Einspritzdüsenkonfiguration als Mittel zur gezielten Beeinflussung der motorischen Gemischbildung und Verbrennung, *Proc. 6<sup>th</sup> Congress on Engine Combustion Processes and Modern Techniques*, pp. 19-30, 2003
2. A.G. MacPhee, M.W. Tate, Ch.F. Powell, Y. Yue, M.J. Renzi, A. Ercan, S. Narayanan, E. Fontes, J. Walther, J.K. Schaller, S.M. Gruner and J. Wang, X-Ray Imaging of Shock Waves Generated by High-Pressure Fuel Sprays, *Science*, Vol. 295, pp. 1261-1263, 2002
3. L. Araneo and C. Tropea, Improving Phase Doppler Measurements in a Diesel Spray, *SAE Paper 2000-01-2047*, 2000
4. G. Smallwood and Ö. Gülder, Views on the Structure of Transient Diesel Sprays, *Atomization and Sprays*, vol. 10, pp. 355-386, 2000
5. H. Harndorf, G. Bittlinger, V. Drewes and U. Kunzi, Analysis of Nozzle Parameters and their Influence on Fuel Mixture Preparation in current and future Diesel Combustion Systems, *Proc. 5<sup>th</sup> International Symposium on Internal Combustion Diagnostics*, pp. 60-72, 2002
6. R. Schodl, A Laser Dual Beam Method for Flow Measurement in Turbomachines, *Proc. ASME*, Paper 74-GT-159, 1974
7. W. Förster, G. Karpinsky, H. Krain, I. Röhle and R. Schodl, 3-Component-Doppler-Laser-Two-Focus Velocimetry Applied to a Transonic Centrifugal Compressor, *Proc. International Symp. on Application of Laser Techniques to Fluid Mechanics*, 2000
8. H. Chaves, M. Knapp, A. Kubitzek and F. Obermeier, High Speed Flow Measurements within an Injection Nozzle, *SPIE*, vol. 2052, *Laser Anemometry Advances and Applications*, 1993
9. Ch. Schugger and U. Renz, Influence of Spray Velocity and Structure on the Air Entrainment in the Primary Breakup Zone of High Pressure Diesel Sprays, *Proc. of ASME Internal Combustion Engine Division Fall Technical Conference*, ICE-Vol. 39, pp. 281-288, 2002
10. H. Kogelnik and T. Li, Laser Beams and Resonators, *Applied Optics*, vol 5, issue 10, pp. 1550-1567, 1966
11. Ph. Leick, G. Bittlinger and C. Tropea, Velocity Measurements in the Primary-breakup region of Diesel Sprays at Elevated Back-Pressures, *Proc. FISITA World Automotive Congress*, p. 353, 2004
12. C. Kirmse, H. Chaves and F. Obermeier, Korrelationsvelocimetrische Untersuchungen des Diesel-Einspritzstrahls einer Common-Rail Einspritzung, *Proc. SPRAY*, pp. 285-293, 2002
13. C. Kirmse, H. Chaves and F. Obermeier, Investigation of Optically Dense Sprays using Correlation Velocimetry, *Proc. DFG-Priority Program Atomization and Spray Processes*, Paper No. 4.2, 2004
14. H. Hiroyasu and H. Miao, Measurement and Calculation of Diesel Spray Penetration, *Proc. ICLASS*, pp. 1413-1420, 2003